energies

MDPI

Article

Experimental Study on the Characteristics of Activated Coal Gangue and Coal Gangue-Based Geopolymer

Weiqing Zhang [1,2], Chaowei Dong [1,2], Peng Huang [2,3,*], Qiang Sun [2,3], Meng Li [1,2] and Jun Chai [1,2]

1 State Key Laboratory of Coal Resources and Safe Mining, China University of Mining and Technology, Xuzhou 221116, China; wq.zhang@cumt.edu.cn (W.Z.); dongchaowei@cumt.edu.cn (C.D.); limeng1989@cumt.edu.cn (M.L.); TS19020003A31@cumt.edu.cn (J.C.)
2 School of Mines, China University of Mining and Technology, Xuzhou 221116, China; 5980@cumt.edu.cn
3 Key Laboratory of the Ministry of Education for Deep Coal Mining, China University of Mining and Technology, Xuzhou 221116, China
* Correspondence: TBH162@cumt.edu.cn

Received: 14 April 2020; Accepted: 14 May 2020; Published: 15 May 2020

Abstract: Coal gangue-based geopolymer (CGGP) is one of the hot spots existing in the recycling of coal gangue resources due to its good comprehensive mechanical properties. However, the coal gangue structure is stable and reactivity is poor, so the coal gangue needs to be activated before utilization. In this paper, the microstructure changes of activated coal gangue by different mechanical and thermal activation methods, as well as the mechanical properties and microstructure changes of the CGGP specimens were studied by experimental investigation. The results indicated that mechanical activation and thermal activation were two effective methods to change the reactivity of coal gangue, which consisted of destroying the stable kaolinite structure and improving the activity of coal gangue. Conversely, part of the amorphous structure in coal gangue was destroyed when the activation temperature reached 900 °C, which was not conducive to the further enhancement of coal gangue activity. For the CGGP prepared by thermally activated coal gangue and modified sodium silicate alkali solution, the uniaxial compressive strength of the CGGP specimens decreased with thermal activation temperatures of the raw coal gangue materials at 700 °C, 800 °C, and 900 °C. The main reason for this was the lower amount of the active metakaolin structure in coal gangue at 900 °C, which was not conducive to the geopolymerization process.

Keywords: coal gangue; geopolymer; mechanical activation; thermal activation; mechanical property; microstructure

1. Introduction

China is one of the large energy producer and consumer countries in the world, mainly relying on coal. Long-term and large-scale development of coal resources lead to massive accumulation of coal gangue [1,2]. In a coal mining environment, the large amount of coal gangue piled up on the ground encroaches the land, and pollutes both the air and water environments [3–5], seriously threatening the ecological security of the mining area and the sustainable development of the coal mining industry. Therefore, resource utilization of coal gangue is urgently required. Coal gangue are mainly reused as supplementary materials in backfilling technology, building construction, energy fuel, soil improvement, water purification, special cementitious materials, etc. [6–8]. Geopolymer is a kind of environmentally friendly mineral polymer material, which has an excellent cementitious property and is a hot topic in the field of industrial solid waste recycling. Geopolymer is an inorganic

polymer mainly produced by the polycondensation of aluminosilicate mineral materials with alkaline solution at room temperature, generally below 100 °C [9,10]. Geopolymer has the characteristics of high strength, fast hardness, high toughness, acid and alkali resistance, high temperature resistance, and other excellent properties. At present, geopolymers are widely used in the fields of green building materials, fire-resistant and high temperature resistant materials, sealing of toxic and dangerous wastes, aerospace materials, etc. [11,12]. The raw materials for preparing geopolymer are mainly composed of silica and alumina, including the natural clay mineral kaolinite, metakaolinite [13,14] and various industrial solid wastes, such as slag, fly ash, red mud, waste glass, and coal gangue [15–18]. The silica and alumina components account for 60–95% of coal gangue so that coal gangue has potential characteristics as a raw material to prepare geopolymer.

However, the coal gangue structure is stable. Its reactivity needs to be improved before use by activation methods, such as mechanically grinding, thermal and chemical activation [19,20]. Different activation methods have different activation effects because of the diversity and complexity of coal gangue. The activated coal gangue can be used alone or combined with other industrial solid wastes for the geopolymer reaction. The calcined coal gangue was mixed with alkaline solutions to prepare amorphous alkali-aluminosilicate cementitious materials, in which the cementitious materials prepared by modified water glass had higher compressive strength [21]. The impacts of sodium hydroxide modulus, alkali lye amount, and liquid–solid ratio on the strength and microstructure of coal gangue geopolymer were explored by Yi, et al [22]. With the increase of sodium hydroxide solution concentration, the strength of geopolymer materials increased, while the mass ratios and liquid–solid ratios did not increase linearly. The spontaneous coal gangue mixed with slag, fly ash, and alkaline solutions was used to prepare the spontaneous combustion gangue-slag-fly ash geopolymer [23,24]. The geopolymer's performance met the standard of Portland cement, and the modulus of water glass; the amount and type of activator can influence its mechanical strength. For coal gangue polymer mortars, the addition of slag and slaked lime improved the compressive strength of geopolymer [25]. The geopolymer recycled concrete was produced by hypergolic or calcined coal gangue, slag, fly ash, and recycled aggregate as raw materials. Its compressive and splitting tensile strengths were high and in line with the engineering requirements of concrete [12]. Other geopolymers with excellent properties were also prepared by coal gangue and thermal activated sludge [26,27] or red mud [28,29]. After adding fly ash, the geopolymer prepared by coal gangue, red mud, and fly ash with sodium silicate solution can reach a compressive strength of 7.3 MPa [30]. In addition, coal gangue can be used as aggregate to be cemented or compounded by other geopolymer materials. A paste filling material was prepared by cementing spontaneous combustion coal gangue with geopolymer, which was prepared by fly ash, cement, slag, and modified sodium silicate [31–33].

As a solid waste resource, coal gangue has potential value in geopolymer research. Recently, most of the researches have focused on experimental research of different material ratios, but the role of each component in the geopolymer preparation process was not completely revealed. This is of great significance for the theoretical guidance of geopolymer preparation using coal gangue. Besides, the activation effect changes with the diversity and complexity of coal gangue. Therefore, this paper mainly studied the microstructure change of coal gangue under different mechanical and thermal activation conditions. The active structural characteristics of activated coal gangue as raw material for preparing geopolymer were summarized. The macro mechanical property and micro structural characteristics of coal gangue-based geopolymer (CGGP) were measured and analyzed for in depth understanding of the polymerization of CGGP.

2. Materials and Methods

2.1. Coal Gangue Sample

Raw coal gangue samples were obtained after washing raw coal from a coal mine in mid-eastern China. The raw coal gangue was broken and screened to 80–100 mesh and dried for 6 h at 30 °C air

environment to obtain the experimental sample, which was named as-received coal gangue, as shown in Figure 1.

(**a**) (**b**)

Figure 1. Coal gangue samples. (**a**) Raw coal gangue; (**b**) As-received coal gangue.

The chemical composition of as-received coal gangue was measured by Bruker S8 Tiger X-Ray Fluorite Spectroscopy (XRF) at a voltage of 50 kV and current of 50 mA with the no-standard quantitative analysis. The loss on ignition was tested according to the international standard ASTM D7348-13. The main chemical compositions and loss on ignition of as-received coal gangue are shown in Table 1. The proximate and elemental analysis (air-dried base) are shown in Table 2.

Table 1. Main chemical composition and loss on ignition of as-received coal gangue (wt%).

Chemical Composition								Loss on Ignition
SiO_2	Al_2O_3	Fe_2O_3	CaO	K_2O	TiO_2	MgO	Na_2O	
45.26	21.62	2.839	2.69	1.65	0.72	0.608	0.415	23.4

Table 2. Proximate and elemental analysis of as-received coal gangue (wt%).

Proximate Analysis				Elemental Analysis				
Ash Content	Volatile	Fixed Carbon	Moisture	Carbon	Oxygen	Hydrogen	Nitrogen	Sulfur
77.76	12.46	8.87	0.91	12.42	7.12	1.27	0.26	0.26

Table 1 shows that the main chemical components of as-received coal gangue were SiO_2 and Al_2O_3, accounting for 66.88%, according to the quantitative analysis results of XRF standard-free samples. Table 2 shows that the ash content of as-received coal gangue was the highest, and the proportions of volatile and fixed carbon were relatively higher as per proximate analysis proportions. On the other hand, the elemental composition analysis showed that the content of carbon element was the highest, followed by that of oxygen.

2.2. Methods and Processes

2.2.1. Activation of As-Received Coal Gangue

The as-received coal gangue was ground by a planetary mill (Instrument type: BM6Pro) continuously for 2 h, 10 h, and 20 h at 400 rpm to obtain mechanical activation coal gangue (named as 2 h-CG, 10 h-CG, and 20 h-CG respectively). Each grinding was carried out in a 250 ml stainless steel pot using 300 g zirconia balls (ball gradation was 116:2198 and weights were 0.86 g and 0.091 g respectively). The three grinding times were chosen according to the reference [19].

The as-received coal gangue after being ground for 2 h was calcined for 2 h at 700 °C, 800 °C, and 900 °C in a tube furnace (Instrument type: MTF 12/38/250/301) to obtain thermal activation coal gangue (named as 700 °C-CG, 800 °C-CG and 900 °C-CG respectively). The three calcination temperatures were determined according to the transformation temperature of the kaolinite structure to active metakaolinite [10].

2.2.2. Preparation of Alkali Medium

A certain amount of water glass (8.5% Na_2O, 26.5% SiO_2, 65% H_2O,) was first mixed with deionized water with magnetic stirring at low speed at 30 °C for 20 min, then slowly poured into a beaker containing a certain amount of 96% sodium hydroxide. The mixture was fully stirred to obtain an even alkali medium of modified sodium silicate with modulus of 1 and solid content of 30%. The alkali medium was used after it cooled to room temperature.

2.2.3. Preparation of CGGP

The preparation process of CGGP was as follows: place the thermally activated coal gangue into a mixing pot, add the alkali medium (mass ratio of liquid to solid was 11:14), and mechanically stir the solid–liquid mixture until it becomes uniform; by this means the CGGP sample was obtained. The sample was filled into a mold with diameter of 50 mm and height of 100 mm, cured at room temperature until it solidified, then removed from the mold and cured continuously for 7 days at 20 °C and 92% relative humidity to obtain the CGGP specimen. The preparation process is shown in Figure 2. The CGGP specimens were named as 700 °C-CGGP, 800 °C-CGGP and 900 °C-CGGP, respectively. The three CGGP specimens, prepared mainly by thermally activated coal gangue and medium alkali, were determined based on the prior knowledge of the importance of the thermal temperature on activation results [10,19] according to sensitivity analysis [34–36].

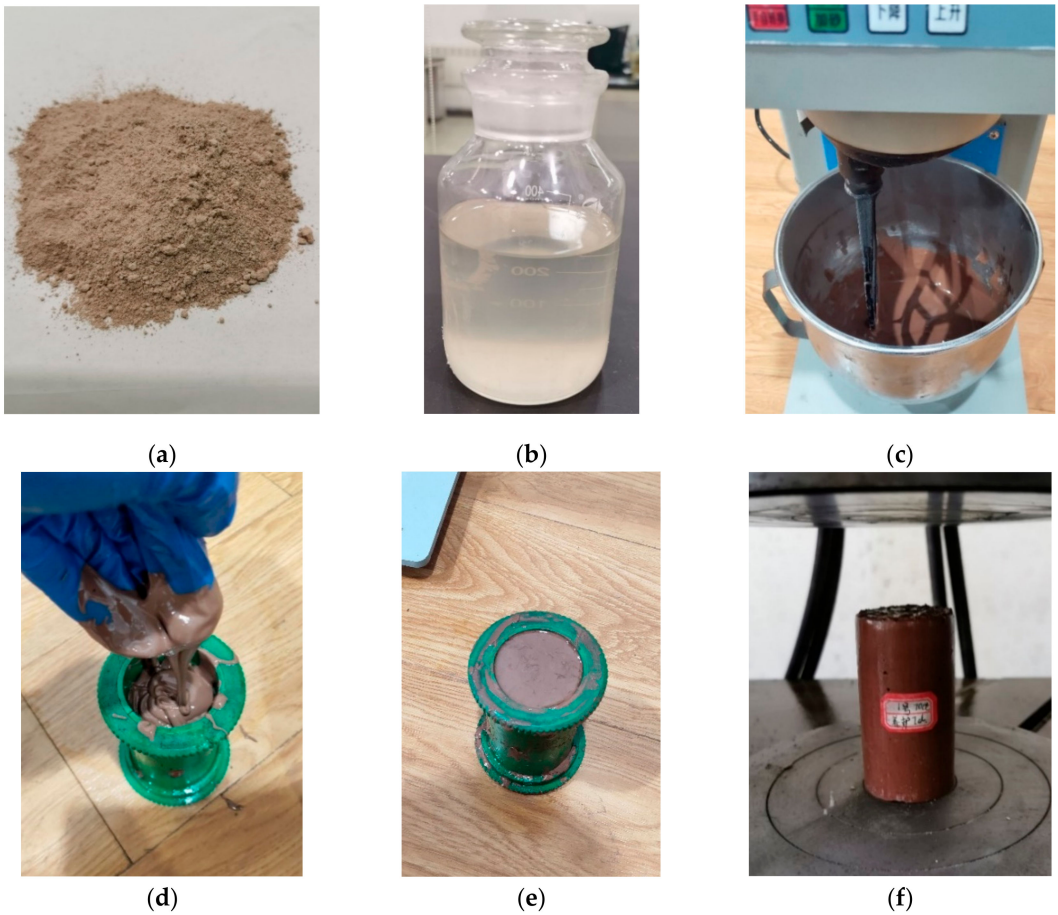

Figure 2. Preparation process of coal gangue-based geopolymer (CGGP) specimen: (**a**) 700 °C-CG; (**b**) Alkali medium; (**c**) Mixing and stirring; (**d**) Filling into mold; (**e**) Solidifying at room temperature; (**f**) Cured 700 °C-CGGP specimen.

2.3. Sample Characterization

The mineral composition was measured by Bruker D8 advance X-Ray Diffraction (XRD) at scanning speed 2°/min and scanned area 5–70° (2θ). Jade 6.5 software was used for interpretation of XRD-patterns. The functional groups were measured by Bruker Vertex 80 v Fourier Transform Infrared Spectroscopy (FTIR) with spectral range of 400–4000 cm^{-1} and resolution of 0.06 cm^{-1}. Omnic software was used for interpretation of FTIR spectra.

The uniaxial compressive strength (UCS) values were tested according to the American Society for Testing Materials (ASTM) by an electro-hydraulic servo universal test machine (Instrument type: WAW-1000D, Changchun Sinter Testing Machine Co., Ltd., China). The displacement rate was 0.05 mm/min. The test for each type of CGGP sample was repeated three times, and its average value was taken as the final UCS.

3. Results and Discussion

3.1. Effect of Mechanical Activation on Coal Gangue Structure

The structure of the silicon–alumina phase in coal gangue, the main raw materials for preparing geopolymer, mainly exists in the form of a stable kaolinite structure. The destruction of the kaolinite crystal structure is an important aspect for coal gangue activation [37]. The XRD spectra of as-received coal gangue and mechanical activation coal gangue are shown in Figure 3.

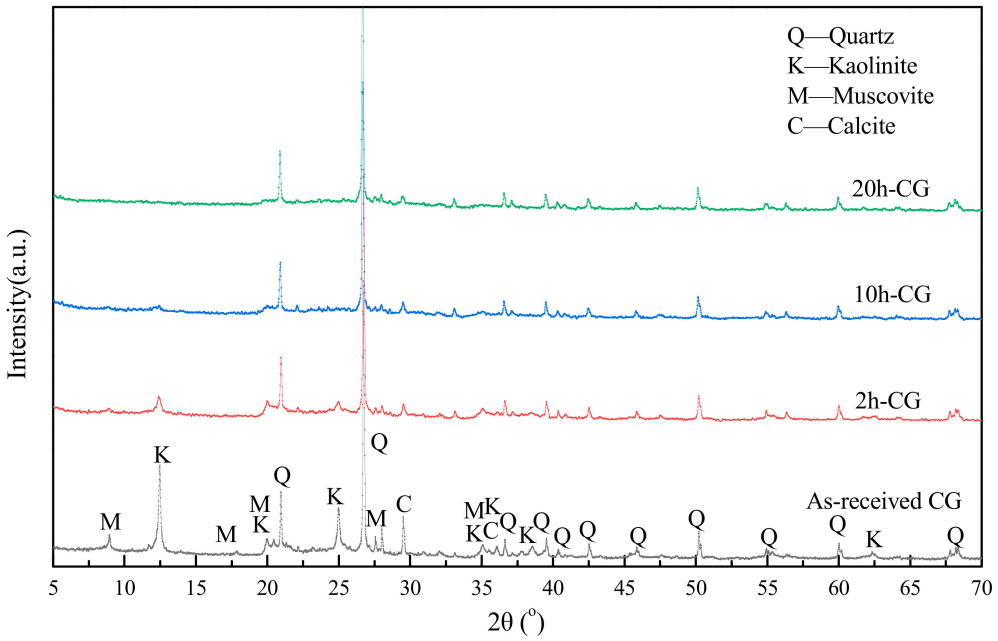

Figure 3. XRD spectra of as-received coal gangue and mechanical activation coal gangue.

Figure 3 shows that the as-received coal gangue was mainly composed of minerals such as kaolinite, quartz, muscovite, and calcite. According to the XRD spectra of raw coal gangue and mechanically activated coal gangue: (1) The intensity of the diffraction peaks at 12.46°, 24.99°, 35.11°, and 38.55° associated with the kaolinite structure decreased significantly after grinding for 2 h, became very weak after grinding for 10 h, and disappeared completely after grinding for 20 h. The intensity reduction of the kaolinite structure indicated that the stable crystal structure of kaolinite in coal gangue can be effectively destroyed by mechanical grinding. (2) The intensity of the diffraction peaks of muscovite at 8.94° and calcite at 29.5° weakened at 2 h grinding and disappeared at 10 h grinding, indicating that the structures of muscovite and calcite were also destroyed. (3) The diffraction peaks of

quartz at 20.96° and 26.73° were stable during the mechanical grinding process and the peak intensities were always significant, which showed that the quartz structure in coal gangue is stable.

The XRD results demonstrated that the mineral crystal structure in coal gangue had been destroyed to different degrees except for quartz under the condition of mechanical activation. An obvious change was observed with the destroyed kaolinite structure, which showed that mechanical activation was conducive to improve the activity of coal gangue.

The structural unit layer of kaolinite in coal gangue is a 1:1 stacked layer composed of Si^{IV}–O tetrahedral layer and Al^{VI}–O octahedral layer, and the stable structural unit layers are linked by hydrogen bonding [38]. Therefore, the removal of the hydroxyl structure in coal gangue can reduce the effect of hydrogen bonding, thus effectively destroying the order of the kaolinite structure and enhancing the activity of coal gangue [39]. The change of the hydroxyl groups can be effectively characterized by FTIR spectra. The FTIR spectra of as-received coal gangue and mechanically activated coal gangue are shown in Figure 4.

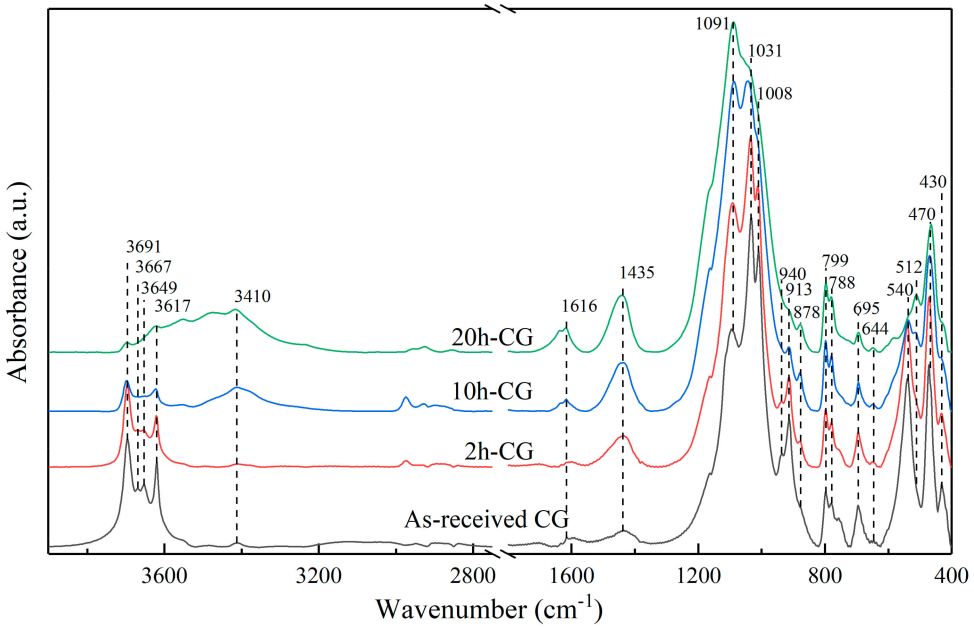

Figure 4. FTIR spectra of as-received coal gangue and mechanically activated coal gangue.

Figure 4 displays that with the increase of mechanical activation time, the peaks in the range of 3800–3200 cm^{-1}, 1200–950 cm^{-1} and 650–400 cm^{-1} changed significantly. According to the FTIR spectra: (1) In the range of 3800–3600 cm^{-1}, the peaks at 3691 cm^{-1}, 3667 cm^{-1}, and 3649 cm^{-1} belong to the inner surface hydroxyl stretching vibration, and the peaks at 3617 cm^{-1} belong to the inner hydroxyl stretching vibration of Al^{VI}–O octahedron [37,40,41]. The broad peak in the range of 3600–3200 cm^{-1} is related to hydrogen bonding of water molecules. With the increase of the mechanical grinding time, the peaks of hydroxyl stretching vibration in the range of 3800–3600 cm^{-1} gradually weakened, while the broad peaks at 3410 cm^{-1} began to increase significantly from 10 h, indicating that with the removal of hydroxyl in the kaolinite structure, adsorbed water gradually formed. After 20 h grinding, only weak absorption peaks of hydroxyl stretching vibration could be observed, while the vibration peaks of hydrogen bonding between water molecules was further enhanced. This showed that the hydroxyl structure in mechanically activated coal gangue decreases and the amount of adsorbed water increases with the increase in grinding time. (2) The peaks at 940 cm^{-1} and 913 cm^{-1} belong to the bending vibration of inner surface hydroxyl and inner hydroxyl, respectively [40,42]. With the increase in mechanical grinding time, the two peaks gradually weakened and disappeared at 20 h, which further confirmed the removal of the hydroxyl structure in mechanically activated coal gangue. At the same time, the changing pattern of the bending vibration peak [22,37] at 1616 cm^{-1} was consistent with that

at 3410 cm^{-1}, which also confirmed the gradual formation of adsorbed water. (3) The Si–O stretching vibration peaks in the range of 1200–950 cm^{-1} were mainly at 1091 cm^{-1}, 1031 cm^{-1}, and 1008 cm^{-1}, which belonged to the different stretching vibration of Si–O–Si in the Si^{IV}–O tetrahedron [43]. With the increase in grinding time, the peaks at 1031 cm^{-1} and 1008 cm^{-1} gradually weakened and disappeared, and the peaks at 1091 cm^{-1} increased significantly, which indicated that the main structure related to Si–O in coal gangue had changed, mainly with the Si^{IV}–O tetrahedral structure partly deformed. Such deformation was mainly caused by the change of bond length and bond angle of the Si^{IV}–O tetrahedron which was affected by the change of the Al–O polyhedral structure. At 20 h, the peak center shifted from 1031 cm^{-1} to 1091 cm^{-1}, indicating the formation of amorphous structure in mechanically activated coal gangue [19]. (4) The peak at 878 cm^{-1} belongs to the tetrahedral structure of Al^{IV}–O [22]. With the increase in grinding time, the peak intensity underwent a gradual increase, indicating the rise of the tetrahedral structure of Al^{IV}–O, which was beneficial to the enhancement of the activity of coal gangue. (5) The peaks at 540 cm^{-1}, 512 cm^{-1} and 430 cm^{-1} are mainly attributed to the bending vibration of Si–O–Al^{VI}, also the contribution from the deformation vibration of Si–O–Si [43]. The peak intensity at 540 cm^{-1} and 430 cm^{-1} decreased with the increase in grinding time and disappeared at 20 h, indicating that the structure of Si–O–Al^{VI} in mechanically activated coal gangue declined. This was caused by the removal of hydroxyl groups. The peak intensity at 512 cm^{-1} increased with the increase in grinding time, enhancing the formation of a new Si–O–Al structure. (6) The peak at 1435 cm^{-1} was attributed to the O–C–O stretching vibration in CO_3^{2-}, which means that coal gangue may contain carbonates [25,44]. With the increase in grinding time, the peak of the spectrum increased, which is believed to be caused by carbonation during the sample grinding process [22]. (7) The deformation vibration of Si–O chains in the range of 800–650 cm^{-1} [38] and the O–Si–O vibration of quartz structure at 470 cm^{-1} had no obvious changes after the mechanical grinding process.

With the increase in mechanical activation time, the inner surface hydroxyl and inner hydroxyl in coal gangue were gradually removed. The Si–O structure changed, the Si–O–Al^{VI} structure decreased and the Al^{IV}–O tetrahedron structure increased. Such changes were conducive to improving the activity of coal gangue.

3.2. Effect of Thermal Activation on the Coal Gangue Structure

The fixed carbon content in coal gangue is not conducive to the enhancement of the activity of coal gangue; this is why the thermal activation method was considered to be more useful to effectively remove the fixed carbon. The XRD spectra of thermally activated coal gangue (named as uncalcined-CG) and non-thermally activated coal gangue are shown in Figure 5.

From Figure 5: (1) The diffraction peaks of the kaolinite crystal structure at 12.46° and 24.99° disappeared completely in the thermally activated coal gangue, indicating that the thermal activation had a significant destructive effect on the kaolinite structure of coal gangue. (2) The diffraction peak of calcite at 29.51° disappeared completely in the thermally activated coal gangue, and this means that thermal activation can effectively destroy the calcite structure in coal gangue. (3) The diffraction peaks of quartz at 20.96° and 26.73° were significant throughout the process of thermal activation, indicating the quartz structure in coal gangue was stable. (4) In the coal gangue thermally activated at 700 °C and 800 °C, new diffraction peaks at 25.58° and 31.46° appeared, but the intensity weakened obviously at 900 °C, indicating that there were new structures in thermally activated coal gangues but these structures were destroyed at higher temperature.

As observed, under the condition of thermal activation, the mineral components in coal gangue except the quartz structure were significantly damaged, which was conducive to the activity change of coal gangue. However, if the thermal activation temperature was too high, part of the new structures in coal gangue were also destroyed, which is not useful for further improvement of coal gangue activity.

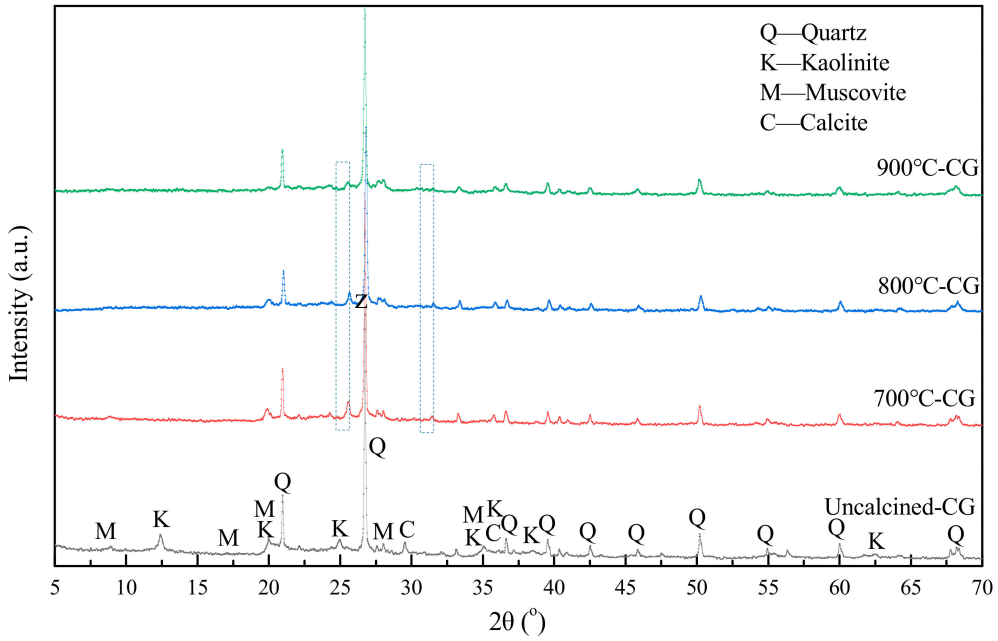

Figure 5. XRD spectra of thermally activated coal gangue and non-thermally activated coal gangue.

The FTIR spectra of thermally activated coal gangue and non-thermally activated coal gangue (also named as uncalcined-CG) are shown in Figure 6.

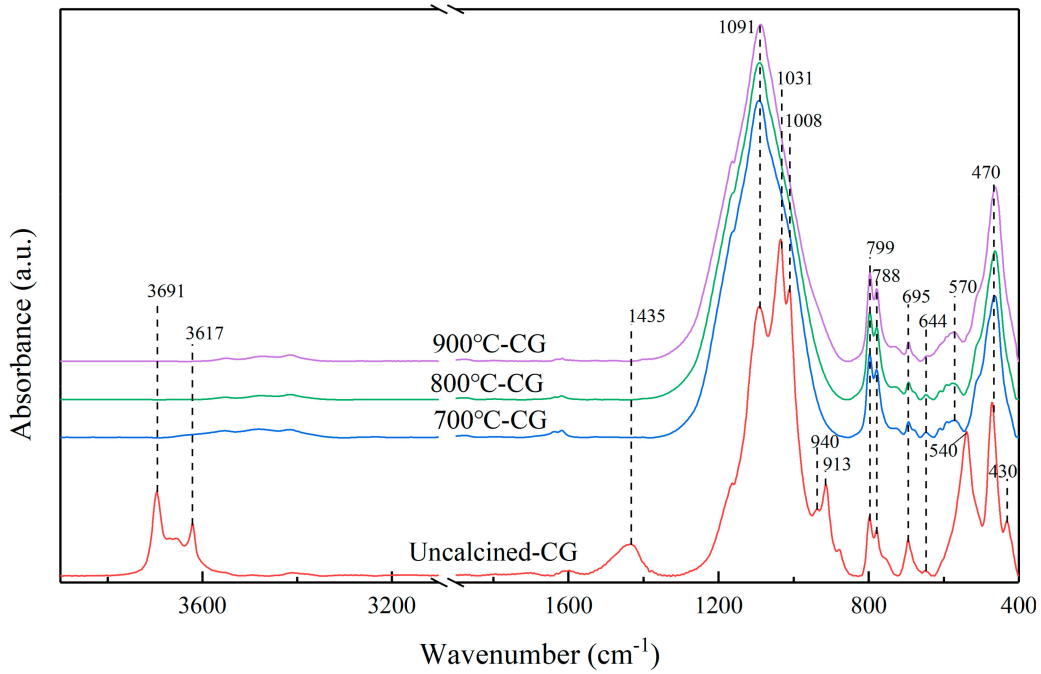

Figure 6. FTIR spectra of thermally activated coal gangue and uncalcined-CG.

From Figure 6: (1) The peak of hydroxyl stretching vibration in the range of 3800–3600 cm^{-1} and the peaks of hydroxyl bending vibration at 940 cm^{-1} and 913 cm^{-1} of thermally activated coal gangue disappeared completely, indicating that the hydroxyl structure in coal gangue can be effectively removed by thermal activation. (2) The stretching vibration peaks of Si–O in the range of 1200–950 cm^{-1} changed significantly. Compared with the uncalcined-CG, the peaks at 1031 cm^{-1} and 1008 cm^{-1} disappeared, while the peak at 1091 cm^{-1} increased and widened significantly, indicating that the main structures related to Si–O in coal gangue changed significantly, especially the crystal kaolinite

structure which changed into the amorphous metakaolinite structure [19]. Such structure changes were similar to those in mechanically activated coal gangue for 20 h grinding time. So, the desired results by thermal activation can be achieved by a sufficiently long mechanical activation process. (3) The peaks of Si–O–Al and O–Si–O in the range of 650–400 cm^{-1} changed significantly. The peaks of Si–O–Al^{VI} at 540 cm^{-1} and 430 cm^{-1} disappeared in the thermally activated coal gangue, and the new peaks of Si–O–Al^{IV} at 570 cm^{-1} appeared. Such results indicated a significant decrease of Al^{VI}–O structure in the kaolinite structure and the formation of a new Al^{VI}–O structure in the metakaolinite structure [19,45]. (4) The complete disappearance of CO_3^{2-} structure at 1435 cm^{-1} after thermal activation indicated the destruction of the carbonate structure in coal gangue, which was consistent with the disappearance of the calcite peak in XRD (Figure 5). (5) There were no obvious changes to the peaks in the range of 800–650 cm^{-1} and 470 cm^{-1}.

Briefly, under the condition of thermal activation, the hydroxyl groups in coal gangue were completely removed and the kaolinite structure was significantly destroyed. The appearance of the Al^{IV}–O structure representing the amorphous metakaolinite structure indicated the improvement of coal gangue activity, so, thermally activated coal gangue can be used as raw material for geopolymer preparation.

3.3. Analysis of Macro- and Micro-Properties of CGGP

The CGGP, with excellent mechanical properties, can be prepared by the geopolymerization of activated coal gangue and alkali medium [10,22]. The UCS is one of the main and most widely used testing methods for the mechanical properties of rocks in mining engineering projects [46,47]. The UCS results of the three CGGP specimens are shown in Figure 7.

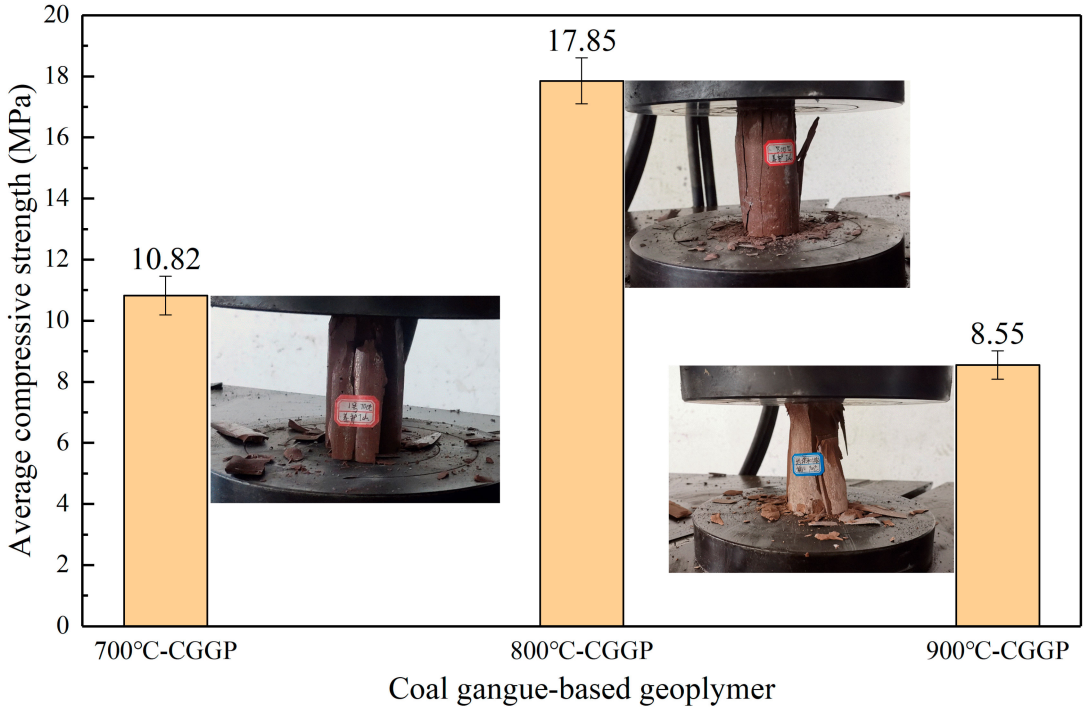

Figure 7. Uniaxial compressive strength (UCS) results of the CGGP specimens.

Figure 7 shows that the average UCS results of the three CGGP specimens fluctuated in the range of 8.55–17.85 MPa, which gives higher UCS results than the previous gangue-cemented paste backfill [48,49]. With the increase in the thermal activation temperature of coal gangue materials, the UCS of CGGP specimens increased first and then decreased. The CGGP specimen prepared by the thermal activation at 800 °C had the largest average UCS, 17.85 MPa, which was 66% (+/−17%) and 110% (+/−21%) higher than those recorded at 700 °C-CGGP and 900 °C-CGGP, respectively.

The main reason was that the presence of more active metakaolinite structures in the thermal activation coal gangue at 800 °C (according to Figures 5 and 6) gave stronger coal gangue reactivity and this became more beneficial to the geopolymerization process. When the temperature increased to 900 °C, part of the active structure in coal gangue was destroyed, resulting in a decrease in coal gangue reactivity [50], which was not conducive to the geopolymerization; thus, the compressive strengths of CGGP specimens were relatively weak. The XRD spectra of CGGP specimens are shown in Figure 8.

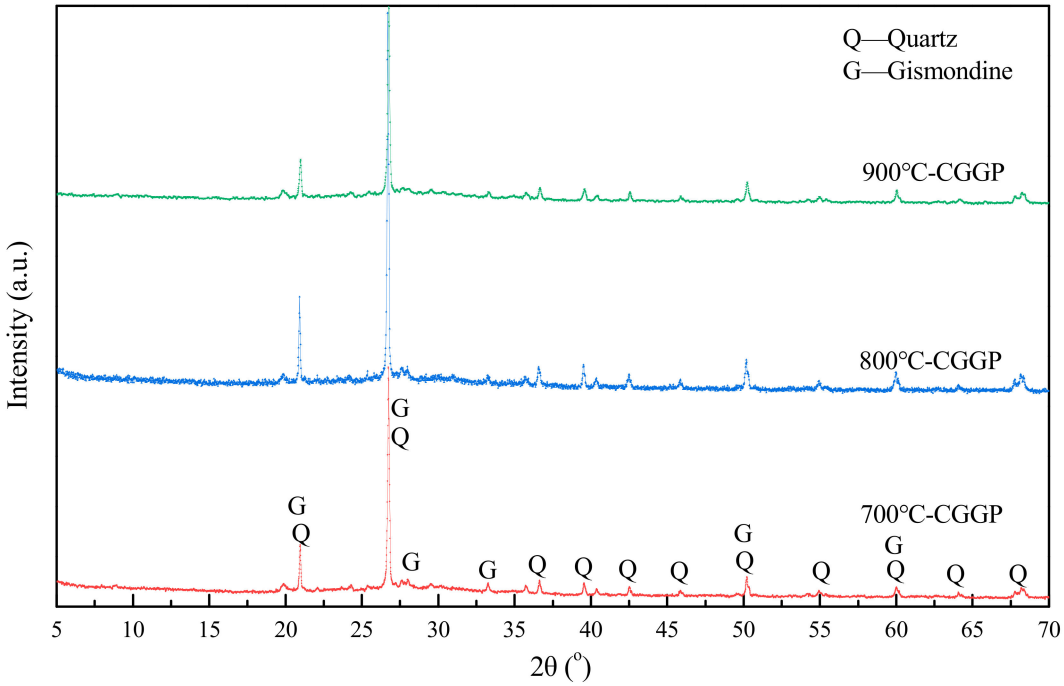

Figure 8. XRD spectra of CGGP specimens.

Figure 8 shows that the crystalline structure of the CGGP specimens was simple, especially the quartz structure. The new diffraction peaks at 25.58° and 31.46° (Figure 5) disappeared in CGGP specimens, indicating that these structures had a great impact in the geopolymerization. The FTIR spectra of CGGP specimens are shown in Figure 9.

From Figure 9: (1) The main peaks of the three CGGP specimens were almost the same, indicating the similarity of the main structures of CGGP. However, compared with the thermally activated coal gangue (700 °C-CG), there were significant changes mainly in the ranges of 3800–3200 cm^{-1} and 1200–950 cm^{-1}. (2) In CGGP, the broad peak of hydroxyl stretching vibration at 3440 cm^{-1} and the bending vibration peak of hydroxyl at 1653 cm^{-1} characterized the chemical binding water generated during geopolymerization [22]. The center of the Si–O stretching vibration spectrum in the range of 1200–950 cm^{-1} shifted from 1085 cm^{-1} to 1011 cm^{-1} and was extended, which was an important point, characterizing the existence of a large number of Si–O–Si and Si–O–Al^{IV} structures in the geopolymer [22,25,30]. The appearance of the Al^{IV}-O tetrahedral structure peak at 878 cm^{-1} confirmed such a conclusion. (3) The difference between the three CGGP peaks was mainly the variation of the peak intensity in the 1200–950 cm^{-1} range. The peak intensity of CGGP prepared by thermal activation of coal gangue at 900 °C was relatively weak at 1011 cm^{-1}, which indicated that the structure of Si–O–Si and Si–O–Al^{IV} in the CGGP structure was less, and the geopolymerization degrees of the 700 °C-CGGP and 800 °C-CGGP were weaker. The peaks of the Al^{IV}–O tetrahedral structure at 878 cm^{-1} were also weakened, which confirmed the same conclusion. So, the new structure in the 900 °C-CGGP was relatively less, resulting in a relatively lower UCS result of the 900 °C-CGGP specimen.

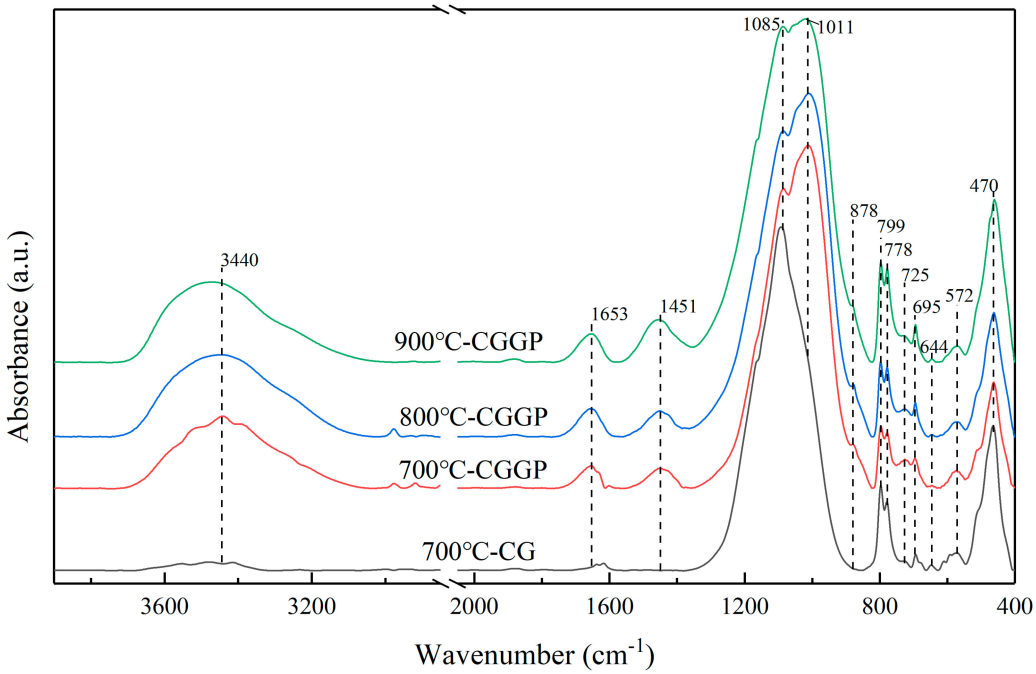

Figure 9. FTIR spectra of CGGP specimens.

In sum, the microstructure of CGGP was significantly different from that of the thermally activated coal gangue, indicating the formation of a new structure in CGGP. The relatively lower content of the new structure was the main reason for the lower UCS result of the CGGP.

4. Conclusions and Future Prospects

In this paper, the microstructure changes of coal gangue activated by different mechanical and thermal activation methods, as well as the macro-mechanical properties and microstructure changes of the CGGP were studied. The main conclusions are as follows:

(1) Mechanical activation and thermal activation are two effective methods for changing the reactivity of coal gangue, whereby both can destroy the stable kaolinite structure and improve the activity of coal gangue. Both FTIR and XRD spectra showed the removal of inner surface hydroxyl and inner hydroxyl, a decrease of Si–O–Al^{VI} structure, and an increase of Al^{IV}–O structure in the activated coal gangue.

(2) The activation effect and microstructure change of coal gangue were different under different activation methods. With the increase in mechanical activation time, the crystal structure of kaolinite in coal gangue decreased and disappeared completely after 20 h grinding. Thermal activation can completely remove the hydroxyl in the kaolinite structure and form the active metakaolinite structure in coal gangue. However, when the activation temperature was too high (900 °C), the new structure in thermally activated coal gangue was destroyed, which was disadvantageous to the further improvement of the coal gangue activity.

(3) The structure of activated coal gangue can be destroyed by the alkaline medium and reconstituted to form CGGP. The UCS results of CGGP prepared by different thermal activations of coal gangue were different. The UCS result of 800 °C-CGGP was the largest, which was higher than those recorded with 700 °C-CGGP and 900 °C-CGGP, respectively. In this paper, results showed that the optimized thermal activation temperature for coal gangue is about 800 °C.

(4) The reason for the lower compressive strength of CGGP was that the active metakaolinite structures were destroyed in thermally activated coal gangue, which led to the decrease of the coal gangue activity and appeared to be a disadvantage for the geopolymerization. FTIR and

XRD spectra showed the formation of new structures in CGGP, while the new structures in CGGP with low compressive strengths were relatively lower.

Coal gangue is a good inorganic material with an aluminosilicate structure for the preparation of geopolymers. Further research work needs to be carried out around the following respects: (1) quantitative analysis of the new structure composition in CGGP to reveal the reaction mechanism; (2) collecting more kinds of coal gangue samples in order to study their activation characteristics using different activation methods; and (3) research on the application of CGGP at the mining engineering site, such as backfilling materials in gob or filling body besides the roadway along the gob in coal mines.

Author Contributions: All of the authors contributed extensively to the present paper. W.Z. and P.H. conceived and provided theoretical and methodological guidance in the research. W.Z. and C.D. designed the experiments, processed and analyzed the data. C.D. and J.C. performed the experiments. M.L., Q.S., and P.H. reviewed and revised the manuscript extensively. All authors have read and agreed to the published version of the manuscript.

Funding: This research was funded by the National Key R&D Program of China (grant number 2018YFC0604704), the Independent Research Project of State Key Laboratory of Coal Resources and Safe Mining, CUMT (SKLCRSM19X001) and the National Natural Science Foundation of China (51704282).

Acknowledgments: We thank the anonymous reviewers for constructive and enlightened comments and suggestions in the revising process.

Conflicts of Interest: The authors declare no conflict of interest.

References

1. Querol, X.; Zhuang, X.; Font, O.; Izquierdo, M.; Alastuey, A.; Castro, I.; Van Drooge, B.L.; Moreno, T.; Grimalt, J.O.; Elvira, J.; et al. Influence of soil cover on reducing the environmental impact of spontaneous coal combustion in coal waste gobs: A review and new experimental data. *Int. J. Coal Geol.* **2011**, *85*, 2–22. [CrossRef]
2. Song, L.; Liu, S.; Li, W. Quantitative Inversion of Fixed Carbon Content in Coal Gangue by Thermal Infrared Spectral Data. *Energies* **2019**, *12*, 1659. [CrossRef]
3. Zhang, J.X.; Ju, Y.; Zhang, Q.; Ju, F.; Xiao, X.; Zhang, W.Q.; Zhou, N.; Li, M. Low ecological environment damage technology and method in coal mine. *J. Min. Strata Contr. Eng.* **2019**, *1*, 1–13.
4. Huang, Y.-L.; Zhang, J.; Yin, W.; Sun, Q. Analysis of Overlying Strata Movement and Behaviors in Caving and Solid Backfilling Mixed Coal Mining. *Energies* **2017**, *10*, 1057. [CrossRef]
5. Querol, X.; Izquierdo, M.; Monfort, E.; Alvarez, E.; Font, O.; Moreno, T.; Alastuey, A.; Zhuang, X.; Lu, W.; Wang, Y. Environmental characterization of burnt coal gangue banks at Yangquan, Shanxi Province, China. *Int. J. Coal Geol.* **2008**, *75*, 93–104. [CrossRef]
6. Li, J.; Wang, J. Comprehensive utilization and environmental risks of coal gangue: A review. *J. Clean. Prod.* **2019**, *239*, 117946. [CrossRef]
7. Zhang, Q.; Zhang, J.; Wu, Z.; Chen, Y. Overview of Solid Backfilling Technology Based on Coal-Waste Underground Separation in China. *Sustainability* **2019**, *11*, 2118. [CrossRef]
8. Huang, P.; Spearing, A.J.S.; Ju, F.; Jessu, K.; Wang, Z.; Ning, P. Control Effects of Five Common Solid Waste Backfilling Materials on In Situ Strata of Gob. *Energies* **2019**, *12*, 154. [CrossRef]
9. Davidovits, J. Geopolymers. *J. Therm. Anal. Calorim.* **1991**, *37*, 1633–1656. [CrossRef]
10. Davidovits, J. Geopolymers Ceramic-Like Inorganic Polymers. *J. Ceram. Sci. Technol.* **2017**, *8*, 335–350.
11. McLellan, B.C.; Williams, R.; Lay, J.; Van Riessen, A.; Corder, G. Costs and carbon emissions for geopolymer pastes in comparison to ordinary portland cement. *J. Clean. Prod.* **2011**, *19*, 1080–1090. [CrossRef]
12. Liu, C.; Deng, X.; Liu, J.; Hui, D. Mechanical properties and microstructures of hypergolic and calcined coal gangue based geopolymer recycled concrete. *Constr. Build. Mater.* **2019**, *221*, 691–708. [CrossRef]
13. Hajjaji, W.; Andrejkovicova, S.; Zanelli, C.; Alshaaer, M.; Dondi, M.; Labrincha, J.; Rocha, F. Composition and technological properties of geopolymers based on metakaolin and red mud. *Mater. Des.* **2013**, *52*, 648–654. [CrossRef]
14. Zhang, H.; Kodur, V.; Wu, B.; Cao, L.; Qi, S.L. Comparative Thermal and Mechanical Performance of Geopolymers derived from Metakaolin and Fly Ash. *J. Mater. Civ. Eng.* **2016**, *28*, 04015092. [CrossRef]

15. Part, W.K.; Ramli, M.; Cheah, C.B. An overview on the influence of various factors on the properties of geopolymer concrete derived from industrial by-products. *Constr. Build. Mater.* **2015**, *77*, 370–395. [CrossRef]
16. He, J.; Zhang, J.; Yu, Y.; Zhang, G. The strength and microstructure of two geopolymers derived from metakaolin and red mud-fly ash admixture: A comparative study. *Constr. Build. Mater.* **2012**, *30*, 80–91. [CrossRef]
17. Zhuang, X.Y.; Chen, L.; Komarneni, S.; Zhou, C.; Tong, D.S.; Yang, H.M.; Yu, W.H.; Wang, H. Fly ash-based geopolymer: Clean production, properties and applications. *J. Clean. Prod.* **2016**, *125*, 253–267. [CrossRef]
18. Mohamad, J.M.; Rassoul, A.; Alborz, H. Preparation and application of alkali-activated materials based on waste glass and coal gangue: A review. *Constr. Build. Mater.* **2019**, *221*, 84–98.
19. Guo, Y.; Yan, K.; Cui, L.; Cheng, F. Improved extraction of alumina from coal gangue by surface mechanically grinding modification. *Powder Technol.* **2016**, *302*, 33–41. [CrossRef]
20. Li, Y.; Yao, Y.; Liu, X.; Sun, H.; Ni, W. Improvement on pozzolanic reactivity of coal gangue by integrated thermal and chemical activation. *Fuel* **2013**, *109*, 527–533. [CrossRef]
21. Zhang, C.S.; Fang, L.M. Hardening mechanisms of alkali activated burned gangue cementitious material. *Mater. Sci. Technol.* **2004**, *12*, 597–601.
22. Cheng, Y.; Ma, H.; Hongyu, C.; Jiaxin, W.; Jing, S.; Zonghui, L.; Mingkai, Y. Preparation and characterization of coal gangue geopolymers. *Constr. Build. Mater.* **2018**, *187*, 318–326. [CrossRef]
23. Zhou, M.; Xu, M.; Li, Z.W.; Sun, Q.W. Preparation and basic properties of spontaneous combustion gangue-slag-fly ash gepolyer. *Bull. Chin. Ceram. Soc.* **2013**, *32*, 1826–1831.
24. Zhou, M.; Wang, C.Z.; Li, Z.W.; Chang, J.; Liu, Q.; Zu, X.J. Ligand optimization of spontaneous combustion coal gangue geopolymer based on the orthogonal and response surface design. *Bull. Chin. Ceram. Soc.* **2013**, *32*, 1258–1263, 1268.
25. Huang, G.; Ji, Y.; Li, J.; Hou, Z.; Dong, Z. Improving strength of calcinated coal gangue geopolymer mortars via increasing calcium content. *Constr. Build. Mater.* **2018**, *166*, 760–768. [CrossRef]
26. Xu, Z.; Zou, X.; Yang, Z. Preparation and Properties of Sludge and Coal Gangue Composite Polymer. *Asian J. Chem.* **2014**, *26*, 1751–1753. [CrossRef]
27. Xu, Z.F.; Zou, X.T.; Chen, J. Preparation of thermal activation sludge and coal gangue polymer. *Integ. Ferroelectr.* **2015**, *160*, 1–9.
28. Geng, J.; Zhou, M.; Li, Y.; Chen, Y.; Han, Y.; Wan, S.; Zhou, X.; Hou, H. Comparison of red mud and coal gangue blended geopolymers synthesized through thermal activation and mechanical grinding preactivation. *Constr. Build. Mater.* **2017**, *153*, 185–192. [CrossRef]
29. Geng, J.; Zhou, M.; Zhang, T.; Wang, W.; Wang, T.; Zhou, X.; Wang, X.; Hou, H. Preparation of blended geopolymer from red mud and coal gangue with mechanical co-grinding preactivation. *Mater. Struct.* **2016**, *50*, 109. [CrossRef]
30. Koshy, N.; Dondrob, K.; Hu, L.; Wen, Q.; Meegoda, J.N. Synthesis and characterization of geopolymers derived from coal gangue, fly ash and red mud. *Constr. Build. Mater.* **2019**, *206*, 287–296. [CrossRef]
31. Sun, Q.; Tian, S.; Sun, Q.; Li, B.; Cai, C.; Xia, Y.; Wei, X.; Mu, Q. Preparation and microstructure of fly ash geopolymer paste backfill material. *J. Clean. Prod.* **2019**, *225*, 376–390. [CrossRef]
32. Sun, Q.; Li, B.; Tian, S.; Cai, C.; Xia, Y. Creep properties of geopolymer cemented coal gangue-fly ash backfill under dynamic disturbance. *Constr. Build. Mater.* **2018**, *191*, 644–654. [CrossRef]
33. Sun, Q.; Cai, C.; Zhang, S.; Tian, S.; Li, B.; Xia, Y.; Sun, Q. Study of localized deformation in geopolymer cemented coal gangue-fly ash backfill based on the digital speckle correlation method. *Constr. Build. Mater.* **2019**, *215*, 321–331. [CrossRef]
34. Reza, A.; Seyed, A.H.; Mojtaba, S.; Abbas, A.S. Updating the neural network sediment load models using different sensitivity analysis methods: A regional application. *J. Hydroinform* **2020**, in press.
35. Andrea, S. Sensitivity Analysis for Importances Assessment. *Risk. Anal.* **2002**, *22*, 579–590.
36. Sobol, I. Sensitivity analysis for non-linear mathematical models. *Math. Model. Comput.* **1993**, *1*, 407–414.
37. Hu, P.; Yang, H. Insight into the physicochemical aspects of kaolins with different morphologies. *Appl. Clay Sci.* **2013**, *74*, 58–65. [CrossRef]
38. Frost, R.L. Hydroxy deformation in kaolin. *Clays Clay Miner.* **1998**, *46*, 280–289. [CrossRef]
39. Ptáček, P.; Frajkorová, F.; Šoukal, F.; Opravil, T. Kinetics and mechanism of three stages of thermal transformation of kaolinite to metakaolinite. *Powder Technol.* **2014**, *264*, 439–445. [CrossRef]

40. Frost, R.L. Combination Bands in the Infrared Spectroscopy of Kaolins—A Drift Spectroscopic Study. *Clays Clay Miner.* **1998**, *46*, 466–477. [CrossRef]
41. Konan, L.K.; Peyratout, C.; Smith, A.; Bonnet, J.-P.; Rossignol, S.; Oyetola, S. Comparison of surface properties between kaolin and metakaolin in concentrated lime solutions. *J. Colloid Interface Sci.* **2009**, *339*, 103–109. [CrossRef] [PubMed]
42. Hamzaoui, R.; Muslim, F.; Guessasma, S.; Bennabi, A.; Guillin, J. Structural and thermal behavior of proclay kaolinite using high energy ball milling process. *Powder Technol.* **2015**, *271*, 228–237. [CrossRef]
43. Castellano, M.; Turturro, A.; Riani, P.; Montanari, T.; Finocchio, E.; Ramis, G.; Busca, G. Bulk and surface properties of commercial kaolins. *Appl. Clay Sci.* **2010**, *48*, 446–454. [CrossRef]
44. Zhu, B.Z.; Sun, Y.L.; Xie, C.W. Spectroscopy research on the Guizhou Xingyi gangue of different calcined temperatures. *J. China Coal Soc.* **2008**, *9*, 1049–1052.
45. Vizcayno, C.; De Gutiérrez, R.M.; Castello, R.; Rodriguez, E.D.; Guerrero, C. Pozzolan obtained by mechanochemical and thermal treatments of kaolin. *Appl. Clay Sci.* **2010**, *49*, 405–413. [CrossRef]
46. Shahri, A.A.; Larsson, S.; Johansson, F. Updated relations for the uniaxial compressive strength of marlstones based on P-wave velocity and point load index test. *Innov. Infrastruct. Solut.* **2016**, *1*, 17. [CrossRef]
47. Asheghi, R.; Shahri, A.A.; Zak, M.K. Prediction of Uniaxial Compressive Strength of Different Quarried Rocks Using Metaheuristic Algorithm. *Arab. J. Sci. Eng.* **2019**, *44*, 8645–8659. [CrossRef]
48. Chen, S.; Du, Z.; Zhang, Z.; Yin, D.; Feng, F.; Ma, J. Effects of red mud additions on gangue-cemented paste backfill properties. *Powder Technol.* **2020**, *367*, 833–840. [CrossRef]
49. Jiang, H.; Fall, M.; Cui, L. Freezing behaviour of cemented paste backfill material in column experiments. *Constr. Build. Mater.* **2017**, *147*, 837–846. [CrossRef]
50. Li, H.; Sun, H.-H. Microstructure and cementitious properties of calcined clay-containing gangue. *Int. J. Miner. Met. Mater.* **2009**, *16*, 482–486. [CrossRef]